

PLAN DE RECHERCHE - Page de couverture
RESEARCH PLAN - Cover Page

Candidat (Prénom, NOM, SCIPER) <i>Candidate (First name, LASTNAME)</i>	Sean THOMAS	217237
Directeur de thèse / <i>Thesis director</i> Codirecteur / <i>co-director</i>	Prof. Yves Perriard	
Nom du laboratoire / <i>Laboratory's name</i> Localisation / <i>Location</i>	Laboratoire d'actionneurs intégrés EPFL	
Date d'immatriculation <i>Date of enrolment</i>	01.09.2017	
Titre provisoire de la thèse <i>Provisional title of the thesis</i>	Smart Grippers : Conception of a novel type of actuator powered by Shape Memory Alloys	
Resumé / Abstract * (max. 3499 caractères espaces inclus/characters incl. spaces)		
The investigation aims to model and conceive a novel type of hybrid gripper striving to serve as a robotic gripper. The gripper will be powered using a hybrid actuator that combines both Shape Memory Alloy (SMA) blades and a bistable system. The thesis will innovate by massively reducing the time response of the SMA so as to offer a light weight and responsive robotic gripper.		

*Résumé et plan de recherche lus et approuvés / * Abstract and research plan read and approved

Candidat <i>Candidate</i>	Directeur de thèse <i>Thesis director</i>	Codirecteur de thèse <i>Thesis co-director</i> Si applicable / If applicable	Dir. de programme <i>Doctoral program dir.</i>
(Date & signature)	(Date & signature)	(Date & signature)	(Date & signature)

Merci de remettre au bureau EDRS ce formulaire dûment complété et signé au plus tard 5 jours après votre examen de candidature.
Please hand in to the EDRS office this form duly completed and signed at the latest 5 days after your candidacy exam.

Contents

1 Name of Candidate and Provisional Thesis Title	1
2 Keywords	1
3 Research Field and Motivation	1
4 State of the Art	2
5 Work Accomplished	8
6 Originality of the Research	14
7 Thesis Plan	14
8 Gantt Diagram	15
9 Publications	15

1 Name of Candidate and Provisional Thesis Title

Candidate Name: Sean THOMAS

Provisional Thesis Title: Smart Grippers: Conception of a novel type of actuator powered by Shape Memory Alloys

2 Keywords

Shape Memory Alloy, Buckled Beam, NiTiNOL, Shape Memory Effect, Bistable system, Self-switching, Modelling and Optimization, Printed Electronics

3 Research Field and Motivation

3.1 Motivation

In an era where manual assembly is no longer possible in the majority of developed countries, it is necessary for companies offering alternative solutions to stand out from their competitors. Manufacturers of assembly lines must modify the capabilities of their robots in order to be as competitive as possible compared to the relocation of the assembly in countries with cheaper labour. In order to stand out, companies such as Mikron SA, seek to increase the efficiency of their installations while preserving the precision appreciated by their customers. The goal of this project would be to conceive and develop a novel and innovative type of Smart gripper. This small part plays a primordial role in the dynamics of the robot. Being at the end of the arm, a small gain in weight of this part would have great consequences on the acceleration and the maximum speed that the robot will be able to reach.

The *Laboratory of Integrated Actuators*, along with a Swiss company, *Mikron SA*, intend to develop a novel type of gripper that will harness the high work output per volume of Shape Memory Alloys (SMA). This gripper would be designed to be lightweight and compact so as to be used as a pick and place gripper in clean room application. The project strives to create an innovative technology that will exploit the characteristics of this smart material to create an actuator that is highly responsive, dynamic, lightweight and compact. These objective will motivate a doctoral thesis that is challenging and innovative.

3.2 Research Field

This project will focus on high response SMA actuation with a large stroke. Currently, few industrial actuators based on SMAs have been seen. This project first has to demonstrate the potential of such actuators as a gripper. Then optimisation of the right topology should reveal the full potential of SMA actuators in terms of time response and stroke. Heating the element is not the greatest challenge, the cooling time of the material must also be taken into account. It is important to note that it is often harder to dissipate heat rather than accumulate it. Thus, various heating and cooling solutions will be exploited and investigated during this project. Another challenge to overcome would be the limited fatigue life of such smart materials. The gripper should at the very least have a fatigue life in the order of 10^6 cycles. The last challenge to over come would be to meet the requirements set by the currently used pneumatic grippers in industry.

This investigation will consider the thermal and mechanical aspect of the material so as to create a highly responsive and dynamic actuator capable of achieving the required force output of traditional grippers. The main focus of the research will be the thermal and

mechanical optimization. The conception of the gripper will include optimization of the geometrical topology of the SMA blades and the use of bistable systems such as buckled beams to create dynamic and high stroke actuators. The command strategies of the actuator will also be an important area of study due to the fact that the actuation of the SMA will involve the precise control of its temperature and resistance.

The symbiosis of the bistable system and the SMA technology can result in an innovative gripper system. The interplay between these two domains will be studied and explored in this thesis.

3.3 Specifications

The specifications of the actuator were obtained by comparing it with the specifications of the Schunk MPG-25 which is the most common pneumatic gripper used in industry, more specifically the primary gripper used by Mikron SA.

Table 1: Specifications of the required actuator

Criteria	Units	Value
Stroke	mm	3
Grip force	N	5
Commutation time	ms	50 - 100
Weight	g	100
Precision/Repeatability	mm	0.02
Number of stable positions	#	2
Volume	mm ³	120

Using the above specifications, the energy that the smart material must supply can be calculated to be approximately 15 mJ. This implies, for example, that for materials such as SMAs, the application would require only a volume of 1.5 mm³.

4 State of the Art

This section will discuss the existing smart materials that are currently studied and used in the domain of actuators. The different techniques and integration systems will also be presented with the goal to compare the various approaches currently used.

4.1 Smart materials

In the field of engineering, ranging from haptics, automation and bio-medical fields, there has been a need to create actuators that are lightweight, compact and having force output. This creates a need for materials that can deliver high forces and strokes while remaining light and small meaning that the materials need to have a high work output.

On the basis of creating an actuator that can meet the demands of the currently implemented strategies while at the same time pushing the limits of the current technology, a thorough investigation of the available smart materials must be conducted. These materials have the ability to react mechanically to an external stimulus such as thermal electrical or magnetic and are thus referred to as *smart* or *active materials*. There exist numerous types of

smart materials and based on their properties, they can be classified into many types based on their activation methods[1].

The aim of this project is to adapt the various smart materials to harness their specific behaviour and fabricate smart actuators. This implies that the system that incorporates the material is equally critical for the conception of the actuator. This section of the report will delve into different strategies used to harness the specific behaviours of the smart materials and integrate them into actuators.

4.1.1 Piezoelectric Materials

Piezoelectric (PZT) materials are a well known type of smart material that reacts to voltages. These materials are already commercially available in various different gripper systems. The company PI[2] is a supplier of PZT actuators and many more such suppliers already exist.

PZT actuators are widely used due to the fact that they have small volumes, high output force ($\sim 10^5 \text{ J/m}^3$) and fast response times (10^6 Hz)[4]. But generally these materials have quite a small maximum stroke, generally around $20 \mu\text{m}$ for a 0.5 mm stack[5]. This implies that PZT actuators will require the integration of amplifiers that will increase the total displacement of the actuator. The work performed by Liang et al., 2018[3] displays a micro-gripper that is comprised of a PZT along with an integrated amplifying system. The study uses flexure-based mechanical structures as an amplifier so as to create a high stroke gripper without a great increase in the total volume of the gripper.

An interested approach to designing the amplification system has been observed in the study performed by Ruiz and Sigmund, 2018[6]. In this work, a large displacement PZT microgripper was designed from a rectangular plate using topology optimization. Here, the PZT plate is sandwiched between two electrodes and an input voltage is applied. This voltage will generate an electric field and will create a deformation in the PZT structure. The optimisation strategy is to increase the deformation by varying the shape and dimensions of the total structure. This strategy could be used in not just this instance but to optimize the actuation of any actuator built around an active smart material.

Based on the literature and the specifications of the gripper, the volume of the piezoelectric material can be calculated to be 150 mm^3 .

4.1.2 Electro-Active polymers

Electroactive Polymers (EAP) have the ability to alter their mechanical behaviour such as a change in shape or size when exposed to an electric field. EAPs emerged in the last few decades exhibiting large strains when exposed to electrical stimulus [7].

EAP can generate high strains, with Dielectric elastomers (DE) such as silicone exhibiting strains of about 63%[8]. EAP materials can also exhibit greater response times, in the order of 10^5 Hz , when compared to smart materials such as shape memory alloys, which will be explored in the next section. EAP can be very useful for their fast actuation times, low density and greater resilience and can, thus, be very convenient when create mechanical devices that are light weight and compact.

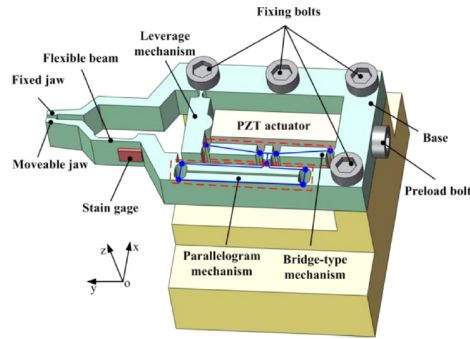


Figure 1: Mechanism of the PZT gripper[3].

The behaviour of the film is caused by the interaction of the electrostatic charges that are created on the opposing electrodes. By applying a voltage on the two electrodes, the electrodes are subjected to opposite charges cause an attractive force between them. The pressure, p , created can be calculated[9] using the following relationship :

$$p = \epsilon_r \epsilon_0 E^2 = \epsilon_r \epsilon_0 (V/t)^2 \quad (1)$$

where ϵ_r and ϵ_0 are the permittivity of free space and the relative permittivity of the polymer respectively, E is the electric field, V is the voltage applied across the electrodes and t is the thickness of the dielectric material.

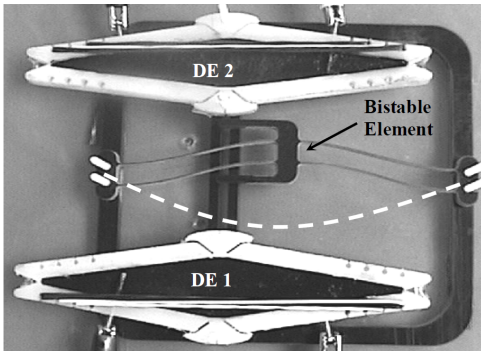


Figure 2: Flip-flop bistable actuator concept[10].

displays DE actuators and a flip-flop bistable mechanism, where two agonistic-antagonistic actuators move a buckled beam back and forth. The DE actuator works as an external trigger mechanism that, when actuated, will force the bistable element into its opposing stable state.

The work shows that the approach to use an antagonistic actuators with a smart material as a trigger mechanism are capable of approximately 10x greater volumetric energy density when compared to traditional flip-flop devices.

Ionic EAP are another variant of EAPs which differ from the DEAP which are sometimes referred to as Electronic EAP[7]. The difference between the two variants arises from the fact that the actuation in Ionic EAPs is a result of diffusion of ions. An interesting Ionic EAP material are Ionic polymer-metal composites (IPMC). These IPMCs are a type of synthetic composite material that has a muscle-like behaviour under an applied voltage or electric field. In figure 3, the working principle is shown where as a voltage is applied, the diffusion of ions within the material causes a deformation. They are generally ionic polymers that are chemically plated with conductors[16].

IPMC bending actuators have been used primarily used as bending actuators and artificial muscles. A novel work conducted by Rossiter et al., 2006[17, 18] where a self-switching strategy is explored within the scope of a buckled bistable beam made entirely of the IPMC smart material. The work addresses many disadvantages experienced by using a classical

Dielectric elastomer (DE) actuators are comprised of an elastomeric film that is platted on both sides with a compliant electrode as shown in figure. The system is actuated when a high voltage is applied between the two electrodes. The main drawback of using DE actuators are the fact that they have very small fatigue life which is around 10^3 cycles[11]. By attempting to use the DE actuators in a continuous fashion, it will result in a short lifetimes and low reliability. In the paper written by Plante et al., 2005[12, 13] or by Wang et al., 2018[14], the teams overcome the burdens of short fatigue life by coupling the DE actuator with a bistable element. Here, the work

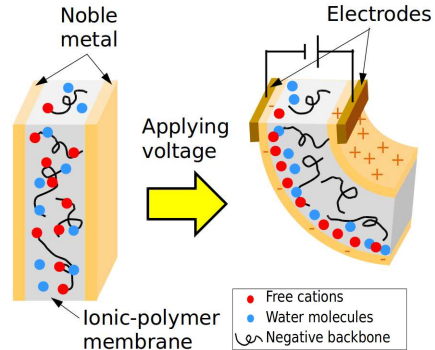


Figure 3: IPMC actuation principle[15].

bistable buckled beam system with an external trigger mechanism such as relaxation after actuation, low repeatability and the need for energy to maintain the stable states. The work concludes that by use of self-switching system, where the material itself is used as the buckled monolithic beam and switches from one stable state to another using applied voltage, the aforementioned disadvantages can be addressed. In this work, a buckled monolithic IPMC beam is separated into a number of electrically independent segments. The work, then, proposes various strategies to activate the segments so as to actuate the beam into transitioning or bifurcating from one of the stable positions to another.

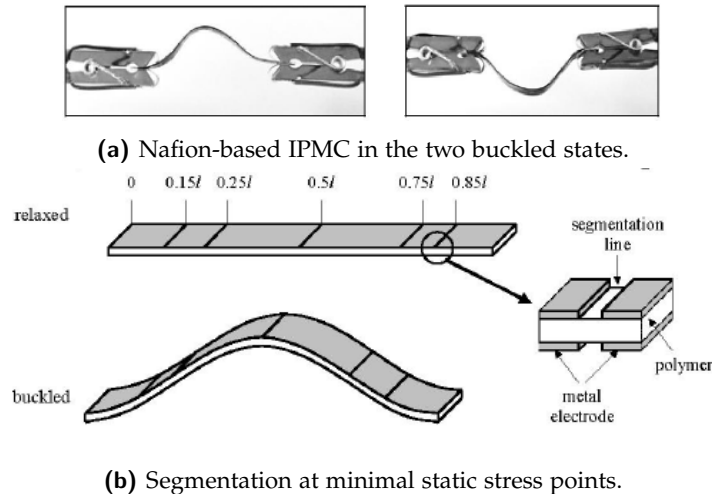


Figure 4: Self-switching IPMC buckled beam[17].

For the purpose of this project, as a means of comparison, the volume of the smart required was calculated. Based on the literature of the energy density and the specifications, the volume required was calculated to be about 20 mm^3 for silicone and about 500 mm^3 for IPMCs.

4.1.3 Magneto-strictive materials

The magneto-strictive materials have the ability to alter their mechanical behaviour and shape when subjected to magnetic fields. Magnetic Shape Memory Alloys (MSMA) are an interesting type of magneto-strictive material. Here, the MSMA shows an interesting behaviour in which the material when deformed will tend to remain stable and retain its deformed shape. As the material is introduced into a strong magnetic field, the crystals of the material are realigned and the material reverts back to its predeformed shape. These MSMAs are an attractive choice as they are capable of high strains around 10% while being able to prove fast response times in the order of 1 kHz[4].

The main drawbacks of MSMAs are the fact that they are quite a new technology implying that they are expensive and that finding suppliers is quite difficult. They are also quite brittle and are thus it makes it quite difficult to find them in different geometries and shapes.

The work presented by Gauthier et al., 2006[19] details the fabrication of a multistable actuator that is based on these MSMAs. Here the device is a push-pull actuator with a pair of agonistic-antagonistic MSMA beams. The active material is actuated using magnetic fields that are created using coils and concentrated using ferromagnetic cores. In figure 5, a working principle of the MSMA actuator can be seen.

The shape memory effect (SME) seen in the MSMA requires the material to be deformed before the application of the magnetic field. Only after the deformation can the strain recover of the SME be observed. In this work, the team was able to create a multistable actuator by using a pair of MSMA. Here, the activation of the first MSMA deformed the opposing beam and vice versa. This results in a displacement and positioning of an end effector placed in between the MSMAs. MSMAs as with traditional SMAs have to be deformed before any actuation can be observed. This work shows the advantages and breakthrough of using an agonistic-antagonistic pair of material to resolve the problem of having to predeform the active material.

One of the important factors that leads to this technology not being widely used, is the fact that the activation of the MSMA requires magnetic fields of around 0.6 T. The work by Lu et al., 2009[20] shows the relationship between strain experienced by the material and the magnetic field density. The work shows an example of a differential rotating MSMA actuator that is powered using permanent magnets and ferromagnetic cores. This study shows that the limiting factor of these technology is the activation magnetic field required for the smart material. The resulting magnetic circuits will render the fabricated actuator to be heavy and bulky. In the use case presented in this work, a rough estimation of the dimensions of the magnetic circuit was established. A basic coil system with dimensions of $23 \times 11 \times 25$ mm would be required to generate the 0.6 T needed for actuation. Thus, the MSMA material will ultimately be unsuitable for the use in small and light weight actuators as desired by this research.

4.1.4 Shape Memory Alloys

Shape memory alloys such NiTiNOL show two important properties: the Shape Memory Effect (SME) and Superelasticity (SE)[21]. SMAs are a particular subgroup of smart materials that change their mechanical behaviour based on a thermal stimulus. Here, the material as with the MSMA, retains its shape when deformed and reverts back to its original shape when heated (SME). Shape Memory Alloys (SMA) actuators provide us with an opportunity to create such actuators due to their high work output per volume which is around 10 J/cm^3 [22]. This can be a 10-fold increase when compared to pneumatic actuators. The SMA actuators are thus able to provide large amounts of force when compared to their volume, making them particularly useful in compact, lightweight actuators.

SMAs are an attractive choice of material for the realisation of small and compact actuators due to their high energy density. They can provide high forces and displacements with a low volume of required material. However, they are thermally activated and have, thus, very long response times. Tomozawa et al.[23], 2005, have worked on fabricating a microactuator using thin film SMA with high transformation temperatures that work at a frequency of 100Hz. The high transformation temperatures and large surface area to volume ratio allows the SMA to cool down and achieve high frequencies. Vitushinsky et al.[24], 2009 have developed also managed to create a highly responsive actuator by reducing the temperature hysteresis seen in SMAs using an actuator that is made up of two SMAs with different transition temperatures.

Paik and Wood[25, 26], 2012 devised a way to decrease the heating time of the SMAs by the way of printed-on coil. In this work, the actuator was fitted with a coil having a higher

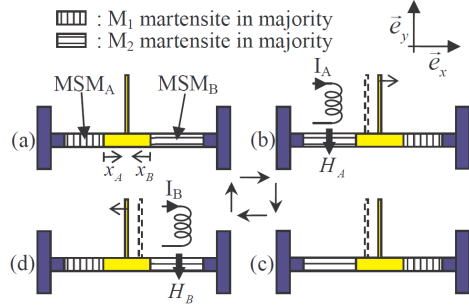


Figure 5: Principle of the actuator[19].

resistivity to further optimize the heating process by Joules heating. The use of an external heating element that was glued to the SMA has decreased the time response by around 30%. Below is a simple heat exchange curve

$$T(t) = (T_A - T_\infty)e^{-t/\tau} + T_\infty, \quad \tau = \frac{C_m \rho V}{hs_{ech}} \quad (2)$$

where C_m is the specific heat capacity, h is the heat transfer coefficient, s_{ech} is the surface area of heat exchange, V is the volume, T_A is the austenitic finish temperature and T_∞ is the ambient room temperature. This equation can be used to calculate the approximate time it would take to cool down the SMA material and thus determine the bandwidth of the material. Using 15 μm thick thin films or 25 μm diameter thin wires and high temperature SMA (around $T_A = 90^\circ\text{C}$), the cooling time can be reduced to 20 ms. A rough estimation of the required SMA for the gripper was calculated to be just around 1.5mm³. Thus, a combination of the innovative ideas proposed in these above works can be used achieve effective results when designing a reactive and compact smart gripper.

4.2 Comparison

The aim of this section of the report is to find the most appropriate type of technology that can replace and innovate the current gripper that are employed in industry. In the current industrial era, most grippers employ the use of pneumatic actuators as their primary source of energy. Thus, to innovate the current domain of gripper, various important factors must be taken into account so as to have a point of comparison between the different smart materials and the presently used pneumatic grippers.

Table 2: Comparison of actuator performances

Actuator type	Stress [MPa]	Strain [%]	Efficiency [%]	Bandwidth [Hz]	Volumetric Work [J/cm ³]
Pneumatic [22]	0.7	50	90	20	0.175
NiTi SMA [22, 27, 4]	200	10	3	10 ²	10
PZT [28, 4]	110	0.1	90	10 ⁶	0.1
MSMA [27, 4, 29]	100	6	90	10 ³	0.15
EAP [28, 4, 27]	3	60	90	10 ⁵	0.75

In the hopes of creating a compact and lightweight actuator, the most important parameter to consider would be the volumetric work. This parameters determines the level at which the active component of the actuator can be minimised when designing the gripper. The SMA offers a great deal better work output to volume ratio when compared to the other materials. The most critical aspect in this case would be attempting to optimize the time response of these SMA in hopes of improving a critical parameter in which this material is lacking.

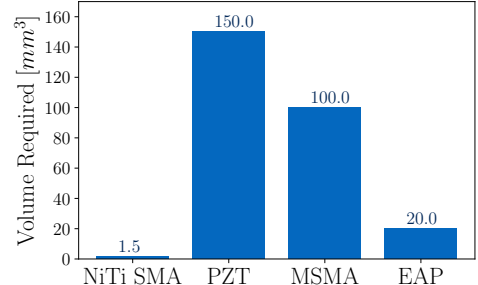


Figure 6: Approximate volume of the smart material required for the gripper based on the specifications and the volumetric work.

5 Work Accomplished

In the previous section, the state of the art explored the various ways in which literature shows the integration of smart materials in actuator systems. Bistable elements using buckled beams shows a lot of promise due to the fact that they do not require energy to maintain the stable position and their potential energy can be used to trigger fast and dynamic strokes. By using the techniques established in the previous section, the SMA can be integrated into a bistable buckled beam system.

5.1 Basic principle of SMA

SMAs exist in various different stable phases which consists of the *Martensitic (M)* phase and the *Austenitic (A)* phase. The M phase can exist in either the *Twinned M phase* or the *Detwinned M phase* based on the stress experienced by the material. The SME is the effect that transforms the material from the A phase to its M phase, also known as the Martensitic transformation. The opposite transformation, from the M phase to the A phase, is known as Austenitic transformation. When the material reaches the Austenitic transformation temperature (A_s) threshold, the material will begin the Austenitic transformation. Inversely, as the material cools down to the Martensitic transformation temperature (M_s), it will begin the Martensitic transformation. Since these transformations occur over a range in temperature, we must heat and cool well beyond the transformation temperatures.

The SMA that in most likelihood will be used is a type of NiTiNOL variant with a relatively high transformation temperature (with A_s around 50°C) and thus exists primarily in the M phase at room temperature. The phase transformations can be seen in figure 7. When a mechanical load is applied to the SMA while in its M phase, the material shears on an atomic level and this allows it to deform through a detwinning process at relatively low stress levels. This process allows the material to deform up to strains of 8%. Strains larger than this will cause dislocations which are irreversible. When the beam is then heated, the Austenite transformation from the detwinned M phase to the A phase, causes the beam to lose all the strain due to twinning, allowing the material to return to its original shape. This strain recovery allows the beam to revert to its pre-defined state while producing large forces.

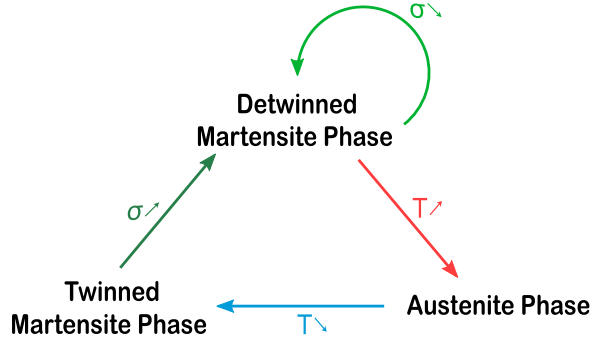


Figure 7: Phase transformation diagram of a shape memory alloy. Here σ represents the stress created by mechanical loading and T represents the temperature change due to thermal loading.

5.2 Buckled beam modelling

When a longitudinal monolithic beam is compressed and the critical axial load is reached, the beam will buckle and result in a bistable structure. The buckled beam will exist in two stable configurations as seen in the figure 8. Specifically, this figure shows the two symmetrical stable states that the buckled beam can exist in for each given stable mode. The figure 9 shows the first three stable modes that are created when a longitudinal beam is pre-compressed.



Figure 8: Stable buckled states of a precompressed beam

When an axial load is applied to the longitudinal beam, the beam reaches a *critical load* and is then deformed sideways, depending on the structure of the beam, to form one of the modes as seen in figure 9. The modes can be described by the equation

$$w = C \left(1 - \cos \left(\frac{(j+1)\pi x}{l} \right) \right), \quad j = 1, 3, 5, \dots \quad (3)$$

which describes the deflection for the odd modes where C is an arbitrary constant, l is the length of the beam and x is the coordinate along the length of the beam. The equation

$$w = C \left[1 - 2 \frac{x}{l} - \cos \left(k \frac{x}{l} \right) + \frac{2 \sin(n_j x/l)}{n_j} \right], \quad k = 2.86\pi, 4.92\pi, 6.94\pi, 8.95\pi, \dots \quad j = 2, 4, 6, \dots \quad (4)$$

describes the deflection of the even modes obtained from [30]. The figure 9 shows the two symmetric stable positions of the buckled beam. The beam can be triggered to switch from one of the states to the other by applying a vertical load at the apex of the curved beam. The displacement of the apex to a critical point will trigger the bifurcation or snap-through and thus the switching of states.



Figure 9: Diagram of the first three buckling modes

The modes seen in figure 9, represent also the transition states of the beam as it transitions from one stable state to the opposing stable state [17]. When a vertical force is applied to the centre of the beam, the buckled beam is forced to transition to the third mode and then finally switches to the opposite state. While if a slight asymmetry is present in the fabrication of the beam or the actuation force, the beam transitions to the second state before switching to the opposite state.

Shape memory alloys can be used to create the buckled beam and can be used to supply the energy required to trigger the bifurcation. Since shape memory alloys can be activated using a thermal load, by applying a current through it, this allows the option to remove the central vertical force required and thus the external triggered required to trigger the switching. Thus, the SMA buckled beam actuation can be deemed a self-switching bistable mechanism. This paper will thus focus on the elimination of the external trigger in regards to standard bistable buckled beam actuators by using the potential energy stored within the SMA material.

5.3 Finite element modelling of SMA

Since the stress distribution in a buckled beam is inhomogeneous, a Finite Element Modelling (FEM) simulation is more suited to handle the complexity of the calculations. The FEM simulation is performed using the Shape Memory Effect material property found in ANSYS Workbench. Using the nine parameters defined in the material property toolbox, we can

simulate the shape memory effect. These parameters were obtained by consulting the material properties established in literature and datasheets from manufacturers[31].

So as to ascertain the reliability of the shape memory effect model created using ANSYS, a simple elongation test was performed. ANSYS workbench was used to model a simple SMA blade and a fractional strain of 8% was applied. The figure 10, shows the evolution of the internal stress of the SMA blade during the ANSYS scenario. This elongation test allows us to create a uniform stressed SMA blade that will perform the same phase changes as seen in the more complex buckled SMA beam.

In figure 10, we can see the various phase changes that occur within the SMA blade. Firstly, one end of the blade is considered a fixed support and has no degrees of freedom. The other end of the blade is subjected to a remote displacement so as to produce a strain. The resulting stress can be observed in region (1) of the figure. As the strain increases, the material reaches its stress threshold to transform from its twinned M phase to its detwinned M phase. This can be observed in region (2), where the strain increases rapidly. Once the blade has reached its maximal strain, the remote displacement is disabled. The region (3) shows that the blade loses its internal stress but remembers the deformation created by the mechanical load. Finally, the SMA blade is heated up and past its transformation temperature and in region (4), the graph shows the strain recovery of the material. The graph shows that after the mechanical load is removed, the SMA retains a small quantity of the internal stress. This inconsistency is due to the way in which the mechanical load is applied to the longitudinal bar within the simulation. The elongation seen in the graph is created using a forced displacement of the edges of the bar. When the elongation is finished and the constraints on the edges are removed, some inconsistencies are seen regarding the internal stress that persist in the material. The material upon heating, immediately returns to zero and the elongation of the bar is recovered. This cycle can be observed in experimental tests studied in literature such as [32, 33]

The FEM simulation was also used to ascertain the volumetric energy density of these SMA material. Here, again a simple monolithic beam was elongated and the work required for this elongation was estimated. Then, as the beam was heated above its transition temperature, the work output due to the strain recovery was measured. The difference between the two values allowed for the verification of the volumetric work presented by the literature shown in table 2.

5.4 Self-switching SMA blade

The next step of the research were to study the effects of geometry optimization to increase the maximal deformation of a buckled SMA beam. The goal is to search for a potential bifurcation of the buckled beam to enhance significantly the displacement. The shape memory effect is only observed in areas of high stress where the material has exceeded the twinning threshold and has attained the twinned M phase as seen in figure 11. Thus during the heating phase, the twinned M phase reverts to the A phase and deformation is observed. Thus, to achieve this twinned state, the SMA beam is pre-constrained by applying a remote displacement to the

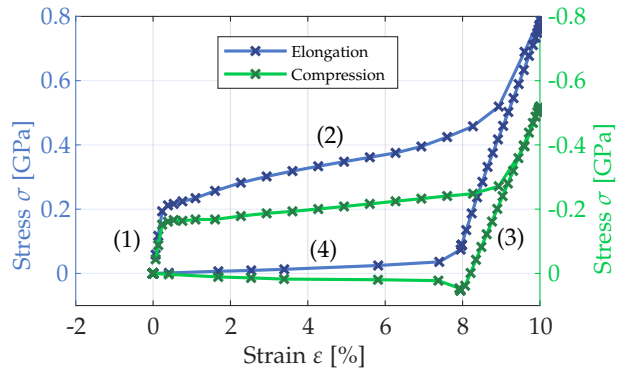


Figure 10: Finite element simulation of SMA Stress-Strain curve in traction and compression using a longitudinal bar

centre vertex while fixing one side face and constraining all but the X axis degree of freedom for the other side face. This step creates a buckled SMA beam which is pre-stressed to allow for the shape memory effect. Finally a thermal load, with a temperature exceeding the transformation temperature, is applied to the structure and the displacement of the centre vertex is recorded.

The strain recovery of the buckled SMA beam can be optimized by increasing the percentage of material that has reached the twinned M phase. This requires the material to be stressed beyond its twinning threshold.

The dimensions of the initial SMA blade is used to optimized the vertex displacement. The strain recovery observed by changing the initial blade dimensions to increase the vertical displacement does not allow for sufficient displacement that would trigger a self-switching. Thus another strategy is required to further improve the strain recovery observed in the buckled beam. An alternative strategy to varying the initial dimensions of the SMA blade would be to add regions of higher thickness to the blade. In figure 12, the thickened region is placed in the centre of the SMA blade. By creating these regions of increased thickness, the SMA blade behaviour can be altered.

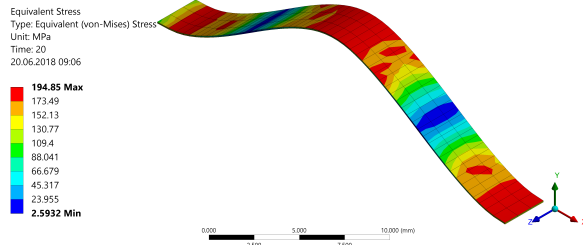


Figure 11: Simulated geometry of buckled SMA blade

Equivalent Stress
Type: Equivalent (von-Mises) Stress
Unit: MPa
Time: 20
20.06.2018 09:06

194.85 Max
173.49
152.13
130.77
109.4
88.041
66.679
45.317
23.995
2.5932 Min

0.000 2.500 5.000 7.500 10.000 (mm)

D: Copy of SMA Center VertDisp
Equivalent Stress
Type: Equivalent (von-Mises) Stress
Unit: MPa
Time: 1
Max: 305.76
Min: 6.3242
20.06.2018 08:54

305.76
272.49
239.22
206.95
173.68
138.41
106.14
72.866
39.595
6.3242

D: Copy of SMA Center VertDisp
Equivalent Stress
Type: Equivalent (von-Mises) Stress
Unit: MPa
Time: 20
Max: 241.85
Min: 1.76
20.06.2018 08:56

241.85
215.18
188.5
161.92
135.14
108.47
81.791
55.114
28.437
1.76

0.000 2.500 5.000 7.500 10.000 (mm)

(a) Before heating

(b) After heating

Figure 12: Stable positions of the buckled beam

The direction in which the blade transitions is due to the convergence of the solution in the simulation. In an experimental scenario, the direction of the transformation can be controlled by creating an asymmetry in the thermal load or mechanical conditions. By applying a thermal load to either direction, the direction of the final stable mode can be chosen.

The creation of a buckled SMA system that can self activate would allow the possibility of creating compact micro-actuators that does not require external activation mechanisms. The goal of the study was to determine and pre-size the parameters that would enable an SMA buckled beam system to behave as a self-switching bistable actuator. This study also offers an overview of the advantages of using finite element modelling to simulate shape memory alloys and the shape memory effect. The work was able to successfully simulate the shape memory effect which corresponds closely to the behaviour of shape memory alloys as seen from experimental trials. The finite element modelling will be an effective tool to create complex actuators using such a material and its shape memory effect behaviour.

The simulations show that the optimization of the dimensions of the initial SMA blade alone cannot provide sufficient strain recovery to transition the buckled beam from one stable mode to another. This is due to the fact that the quantity of the material that transforms

to the detwinned M phase due to the buckling is not sufficient to create enough vertical displacement so as to self-switch.

The work initially strived to vary arbitrary parameters so as to observe an effect on the vertical displacement and thus, subsequently the beams ability to self-actuate. The initial simulations conclude that the parameters that influence the self-switching are difficult to pinpoint. In figure 12b, the stable mode after heating can be observed. The simulations show that by creating a blade with variable thickness, the behaviour of the system can be greatly affected. The thickened regions divide the beam into segments, allowing regions of the beam which are curved in the same direction to be actuated while regions that are curved in the opposite direction to not be actuated. This effect has been seen in [17] where the same principle is used for electrically stimulated self-switching buckled beams. The segmentation allows regions that will actuate in opposite directions to be reduced and thus further improve the vertical displacement.

5.5 Test bench layout

The test bench that was designed to measure the time response of the SMA actuator is constructed as shown in figure 13.

An SMA blade is fixed between two electrodes which allow an electrical current to flow through the system. In this setup, the right electrode is part of the main body of the test bench while the left electrode is placed on a linear guide in order for it to be able to move unidirectionally only. Using this mobile part, the blade is preconstrained while in its M phase i.e. at low temperature. A force sensor is then placed behind the left electrode and fixed to the bench to measure the force applied by the SMA actuator while it tries to return to its initial shape during the transition from the M phase to the A phase, i.e. heating.

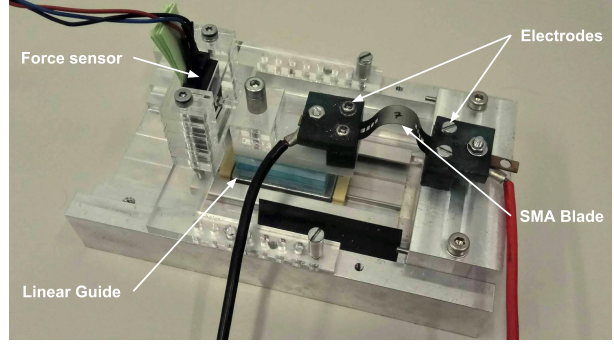


Figure 13: Layout of the test bench

5.6 Thermal response enhancement

The aim of this work is to optimize the heating of the SMA in critical sections and thus improve the force output and actuation times of the SMA actuator. The SMA blades are actuated using Joule heating where a current is passed through the blade and the internal resistance is used to heat the blade. Thus, the geometry of the blade is critical when optimizing the time response of the shape memory effect. The design of the SMA blades were created based on four factors as defined below and shown in figure 14 while also keeping the volume of material used constant:

Factor x_1 : Number of perforations along the width

Factor x_2 : Position of the holes along the length

Factor x_3 : Number of perforations along the length

Factor x_4 : Orientation of the perforation

The volume of material of the blade was also kept constant so as to have the same quantity of material to be heated during each run. This is controlled by ensuring that the thickness of blades are the same and that the total surface area is constant between each blade.

The conventional option for the design of the test would be to design changes in the beam based on one factor at a time and observe the effect on the time response. This method is inefficient and time-consuming. Furthermore, the material is quite expensive, so extracting quality information for multiple construction factors from each blade is primordial. Thus a systematic design based on a Hadamard matrix that changes several variables simultaneously is performed. This allows to perform the analysis of the factor with respect to the time response in terms of the force-time derivative while reducing the number of runs and the quantity of material used.

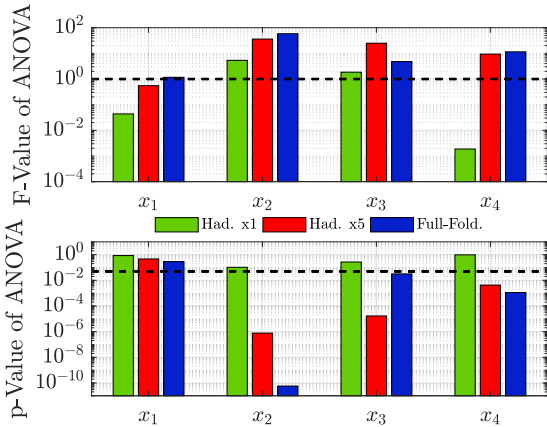


Figure 15: Graph showing the influence of each factor with respect to the residual of the models and the corresponding confidence values.

the ANOVA p-value, which is the probability of having validated a hypothesis by chance. In this case, the hypothesis is that factors have a non-zero influence in the model; meaning that small p-values (being sure that the parameters have a non-null influence) are desirable. As an arbitrary threshold, it was deemed that concluding results should have $p\text{-values} \leq 0.05$ (marked in plot).

After the Had. x1, only x_2 and x_3 were slightly more significant than the residual of the model. Still, their p-values reflected a non-satisfactory certainty upon this affirmation, so it was decided to test the blades four additional times, leading to Had. x5. This time x_2 and x_3 became more influential, whereas x_4 newly became influential. Given their corresponding p-values, it could be affirmed that these three factors indeed affect the force vs time of SMAs; the longitudinal centring of the perforations, the number of them and their orientation, respectively.

Despite the Had. x5 approach, it was not clear if factor x_1 had small or no influence at all in the SMA performance. To gain further insight, and de-alias the results, eight new blades

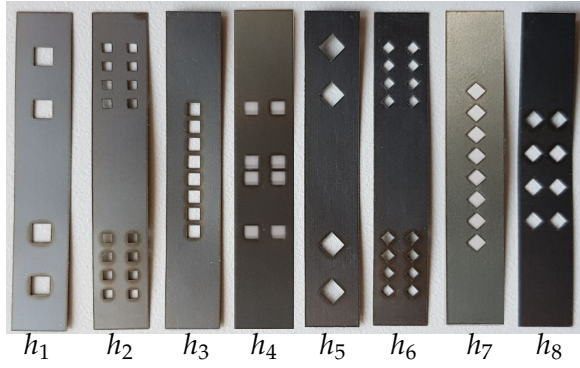


Figure 14: Laser cut SMA blades based on the generated Hadamard matrix and the four factors.

A linear fit of the force derivative with respect to time $\frac{dF}{dt}$ was performed, in the form of $\frac{dF}{dt} \sim x_1 + x_2 + x_3 + x_4$ (in Wilkinson notation) for the Hadamard with one run, five runs, and the full fold-over. To check the significance of the SMA design parameters and their corresponding certainty, an Analysis of Variance (ANOVA) of this model is conducted.

The upper plot of figure 15 represents the ANOVA F-Value: the influence of each factor upon the experiment with respect to the residual of this model. It is desirable to obtain coefficients whose significance is high with $F\text{-value} \geq 1$. The lower plot represents

corresponding to the $-H$ experimental matrix were tested five times each, resulting in a full fold-over design. This analysis confirmed with high certainty the influence of factors x_2 , x_3 and x_4 . This time, however, it claimed a rather non-null influence of factor x_1 , i.e. bigger than measurement noise. Nevertheless, the 0.28 p-value of factor x_1 indicates that the previous affirmation is inconclusive, and that this high influence might be product of randomness. This seems plausible given the very low F-values for factor x_1 and their evolution with the experimental procedures.

In conclusion, this work showed that the response of a SMA blade in terms of maximal force-time derivative can be optimized by carefully placed perforations. Indeed, an improvement by a factor of 3 could be observed between the highest and the lowest response in this experiment. Significant factors could be identified using a Hadamard matrix for the preparation of the samples and an ANOVA analysis of the results. The most relevant factor turned out to be the position of the perforations along the blade, followed by their longitudinal number and orientation.

6 Originality of the Research

The originality of this work lies in the pursuit of designing a gripper system that can harness the high work output of shape memory alloys. The gripper will be inspired by the various innovative smart technology explored within the state of the art. The state of the art shows that there exists many novel ideas for compact, light weight actuators using smart materials but none that are capable of delivering the high work output seen in SMAs. By harnessing the strengths of the SMA and the innovative strategies used in other smart material actuator systems, this research aims to explore the capabilities of the SMA material and develop an innovative gripper system. The following topics are expected to be studied over the course of this research project :

1. Investigation of the SMA capabilities through the study of an analytical and finite element model
2. Optimization of the topology of the active material component in the system for increased performances
3. Optimization of heating and cooling strategies of the SMA so as to decrease response times and bandwidth
4. Design and integration of a bistable system that incorporates an active smart material such as an SMA to achieve a responsive and powerful gripper system

7 Thesis Plan

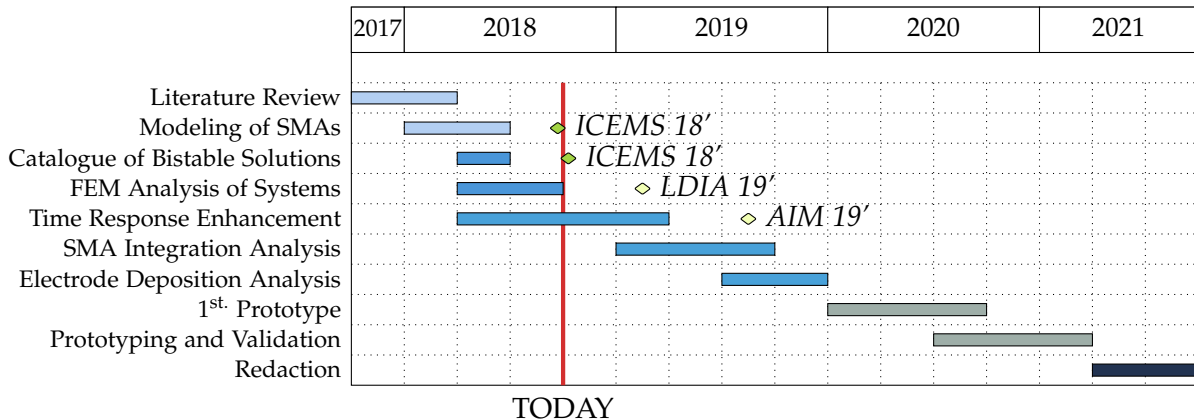
The following list presents a non-definitive thesis plan :

1. Motivation of the thesis
2. State of the art : smart materials and actuation structures
3. Integration of SMAs into bistable systems
4. Enhancement of time responses and deposition techniques of electrodes
5. Prototyping and validation

6. Conclusion

8 Gantt Diagram

The follow diagram proposes a 4-year course for the doctorate. Some relevant conferences are displayed within the diagram.



9 Publications

- Accepted: S. Thomas, M. Almanza, Y. Civet, and Y. Perriard, "Actuation Displacement Analysis of a Self-Switching Shape Memory Alloy Buckled Beam", in *International Conference on Electrical Machines and Systems*, Jeju, 2018, p. 7.
- Accepted: S. Thomas, P. Peralta, R. Mottet, M. Lehmann, Y. Civet, and Y. Perriard, "Analysis and Reduction of Time Response in Thermally Activated Shape Memory Alloys", in *International Conference on Electrical Machines and Systems*, Jeju, 2018, p. 6.

References

- [1] J. Damodharan, A. Sreedharan, and T. Ramalingam, "A Review on Smart Materials, Types and Applications," *International Journal of Engineering Technology Science and Research*, vol. 5, p. 5, Mar. 2018.
- [2] "P-604 Compact PiezoMove Linear Actuator Datasheet," Apr. 2018.
- [3] C. Liang, F. Wang, B. Shi, Z. Huo, K. Zhou, Y. Tian, and D. Zhang, "Design and control of a novel asymmetrical piezoelectric actuated microgripper for micromanipulation," *Sensors and Actuators A: Physical*, vol. 269, pp. 227–237, Jan. 2018.
- [4] E. Faran and D. Shilo, "Ferromagnetic Shape Memory Alloys Challenges, Applications, and Experimental Characterization," *Experimental Techniques*, vol. 40, pp. 1005–1031, June 2016.
- [5] S. J. Rupitsch, *Piezoelectric Sensors and Actuators: Fundamentals and Applications*. Topics in Mining, Metallurgy and Materials Engineering, Berlin Heidelberg: Springer-Verlag, 2019.

- [6] D. Ruiz and O. Sigmund, "Optimal design of robust piezoelectric microgrippers undergoing large displacements," *Structural and Multidisciplinary Optimization*, vol. 57, pp. 71–82, Jan. 2018.
- [7] Y. Bar-Cohen, "Artificial muscles using electroactive polymers (EAP): capabilities, challenges and potential," 2005.
- [8] R. D. Kornbluh, R. Pehrline, H. Prahlad, and R. Heydt, "Electroactive polymers: an emerging technology for MEMS," in *MEMS/MOEMS Components and Their Applications*, vol. 5344, pp. 13–28, International Society for Optics and Photonics, Jan. 2004.
- [9] P. Thummala, L. Huang, Z. Zhang, and M. A. E. Andersen, "Analysis of Dielectric Electro Active Polymer actuator and its high voltage driving circuits," pp. 458–461, IEEE, June 2012.
- [10] J.-S. Plante, M. Santer, S. Dubowsky, and S. Pellegrino, "Compliant Bistable Dielectric Elastomer Actuators for Binary Mechatronic Systems," pp. 121–126, Jan. 2005.
- [11] Y. Chen, R. Vertechy, and M. Fontana, "Preliminary results on the fatigue life characterization of a styrenic dielectric elastomer (Conference Presentation)," in *Electroactive Polymer Actuators and Devices (EAPAD) 2017*, vol. 10163, p. 101630F, International Society for Optics and Photonics, May 2017.
- [12] J.-S. Plante and S. Dubowsky, "On the properties of dielectric elastomer actuators and their design implications," *Smart Materials and Structures*, vol. 16, no. 2, p. S227, 2007.
- [13] P. Chouinard and J. Plante, "Bistable Antagonistic Dielectric Elastomer Actuators for Binary Robotics and Mechatronics," *IEEE/ASME Transactions on Mechatronics*, vol. 17, pp. 857–865, Oct. 2012.
- [14] N. Wang, C. Cui, B. Chen, and X. Zhang, "Design and Analysis of Bistable Dielectric Elastomer Actuator with Buckling Beam," in *MARSS*, (Japan), p. 6, July 2018.
- [15] L. P. Poubel, *Proposal of a Novel Method for Oscillating IPMCs with DC Input*. PhD thesis, Chiba University, Japan, 2011.
- [16] M. Shahinpoor, Y. Bar-Cohen, J. O. Simpson, and J. Smith, "Ionic polymer-metal composites (IPMCs) as biomimetic sensors, actuators and artificial muscles - a review," *Smart Materials and Structures*, vol. 7, no. 6, p. R15, 1998.
- [17] J. Rossiter, B. Stoimenov, and T. Mukai, "A Self-switching Bistable Artificial Muscle Actuator," in *2006 SICE-ICASE International Joint Conference*, pp. 5847–5852, Oct. 2006.
- [18] J. Rossiter, B. Stoimenov, and T. Mukai, "A Bistable Artificial Muscle Actuator," in *2006 IEEE International Symposium on MicroNanoMechanical and Human Science*, pp. 1–6, Nov. 2006.
- [19] J.-Y. Gauthier, A. Hubert, J. Abadie, C. L'Excellent, and N. Chaillet, "Multistable actuator based on magnetic shape memory alloy..," in *Proceedings of the 10th International Conference on New Actuators, ACTUATOR'06.*, vol. 1, (Bremen, Germany), pp. 787–790, June 2006.
- [20] J. Lu, Z. Liang, and W. Qu, "Optimal Design of Rotating Actuators Made by Magnetically Controlled Shape Memory Alloy," in *2009 Ninth International Conference on Hybrid Intelligent Systems*, vol. 1, pp. 95–98, Aug. 2009.

- [21] A. Rao, A. R. Srinivasa, and J. N. Reddy, *Design of Shape Memory Alloy (SMA) Actuators*. SpringerBriefs in Applied Sciences and Technology, Cham: Springer International Publishing, 2015.
- [22] J. Mohd Jani, M. Leary, A. Subic, and M. A. Gibson, "A review of shape memory alloy research, applications and opportunities," *Materials & Design* (1980-2015), vol. 56, pp. 1078–1113, Apr. 2014.
- [23] M. Tomozawa, K. Okutsu, H. Y. Kim, and S. Miyazaki, "Characterization of High-Speed Microactuator Utilizing Shape Memory Alloy Thin Films," 2005.
- [24] R. Vitushinsky, S. Schmitz, and A. Ludwig, "Bistable Thin-Film Shape Memory Actuators for Applications in Tactile Displays," *Journal of Microelectromechanical Systems*, vol. 18, pp. 186–194, Feb. 2009.
- [25] J. K. Paik and R. J. Wood, "A bidirectional shape memory alloy folding actuator," *Smart Materials and Structures*, vol. 21, no. 6, p. 065013, 2012.
- [26] J. K. Paik, E. Hawkes, and R. J. Wood, "A novel low-profile shape memory alloy torsional actuator," *Smart Materials and Structures*, vol. 19, no. 12, p. 125014, 2010.
- [27] G. Rizzello and L. Riccardi, "An Overview on Innovative Mechatronic Actuators Based on Smart Materials," *IEEE Africon 2017 Proceedings*, p. 6, 2017.
- [28] R. D. Kornbluh, R. Pelrine, Q. Pei, R. Heydt, S. Stanford, S. Oh, and J. Eckerle, "Electroelastomers: applications of dielectric elastomer transducers for actuation, generation, and smart structures," in *Smart Structures and Materials 2002: Industrial and Commercial Applications of Smart Structures Technologies*, vol. 4698, pp. 254–271, International Society for Optics and Photonics, July 2002.
- [29] H. E. Karaca, I. Karaman, B. Basaran, Y. Ren, Y. I. Chumlyakov, and H. J. Maier, "Magnetic Field-Induced Phase Transformation in NiMnCoIn Magnetic Shape-Memory AlloysA New Actuation Mechanism with Large Work Output," *Advanced Functional Materials*, vol. 19, pp. 983–998, Apr. 2009.
- [30] S. P. Timoshenko, J. M. Gere, and W. Prager, "Theory of Elastic Stability, Second Edition," *Journal of Applied Mechanics*, vol. 29, no. 1, p. 220, 1962.
- [31] K. Divringi and C. Ozcan, "Advanced Shape Memory Alloy Material Models for ANSYS," tech. rep., Ozen Engineering Inc, 2009.
- [32] O. Hongchun Xie, "Design, simulation and experimental study of shape memory alloy and micro-motor activated high pressure optical cell for bio-physical studies," p. 180, Oct. 2007.
- [33] Y. Liu, Z. Xie, J. Van Humbeeck, and L. Delaey, "Asymmetry of stressstrain curves under tension and compression for NiTi shape memory alloys," *Acta Materialia*, vol. 46, pp. 4325–4338, July 1998.